Polymer Chemistry

PAPER

View Article Online
View Journal | View Issue

Cite this: *Polym. Chem.*, 2019, **10**, 2570

Diblock copolymers consisting of a redox polymer block based on a stable radical linked to an electrically conducting polymer block as cathode materials for organic radical batteries†

Noémie Hergué, *[a] Bruno Ernould,[b] Andrea Minoia,[c] Julien De Winter,[d] Pascal Gerbaux,[d] Roberto Lazzaroni,[c] Jean-François Gohy,[b] Philippe Dubois[a] and Olivier Coulembier[a]

Received 18th February 2019,
Accepted 14th April 2019

DOI: 10.1039/c9py00268e

rsc.li/polymers

End-functionalized poly(3-hexylthiophene) (P3HT) and poly(2,2,6,6-tetramethylpiperidinyloxy-4-yl methacrylate) (PTMA) were synthesized using controlled polymerization techniques and linked together to lead to a diblock copolymer structure *via* click cycloaddition. These diblock copolymers were further blended with carbon nanotubes (CNTs) to be used as cathodes in organic radical batteries. The performances of these batteries were studied during charge/discharge cycling at constant and variable current densities (C rate). In order to shed light on the importance of the diblock copolymer architecture, the results were compared to the capacities measured on electrodes made of blends of P3HT and PTMA homopolymers. Theoretical simulations were finally used to corroborate the good electrochemical properties of the synthesized diblock copolymers.

Introduction

In the field of energy storage, the development of organic radical batteries (ORBs) is showing promising advances.[1,2] Indeed, this technology is combining the advantages of both lithium-ion batteries (LiBs),[3] *i.e.* high energy densities, and supercapacitors, *i.e.* high power.[4] The principle of this technology lies in the use of highly reversible and fast redox reactions associated to some organic groups. In this context, organic molecules containing the so-called stable organic radicals have shown very interesting redox properties when incorporated in batteries as cathode materials.[5] Therefore, several organic molecules incorporating organic radicals were developed where the radical is located either on a nitrogen (diphenylpicrylhydrazyl[2]) or an oxygen atom (galvinoxyl,[6] phenoxyl,[7] nitroxide[8]). Among the stable radicals reported so far, the oxygen-centered (2,2,6,6-tetramethylpiperidin-1-yl)oxyl (TEMPO) radical is demonstrating promising electrochemical properties, but cannot be simply used as a molecular material in ORBs due to its high solubility in battery electrolytes. To decrease their solubility, TEMPO units have been incorporated as pendant groups onto a polymethacrylate backbone leading to the poly(2,2,6,6-tetramethylpiperidinyloxy-4-yl methacrylate) (PTMA) redox polymer. This polymer, introduced in ORBs by Nishide and coworkers in 2004,[9] is receiving a high interest due to its two reversible redox processes. At 3.6 V *vs.* Li/Li^+, the nitroxide radicals of PTMA are oxidized into oxoammonium cations while they are reduced into aminoxyl anions at 2.6 V *vs.* Li/Li^+.[10] PTMA also presents a combination of good properties for battery application such as: a high-power capability, a theoretical capacity of 111 mA h g^{-1}, a fast charging and a radical stability leading to high stability during cycling.[9] However, the electrical conductive properties of PTMA are too low for the material to be used as a pure component and the addition of a conductor is essential. PTMA has thus been blended with different conductors such as carbon nanotubes (CNTs),[11,12] graphene[13] and graphene oxide[14] sheets. However, the corresponding electrodes are showing a decrease of the capacity upon cycling due to a progressive solubilization of the polymer into the electrolyte. To avoid such migration, it is

[a]*Laboratory of Polymeric and Composite Materials (LPCM), Center of Innovation and Research in Materials and Polymers (CIRMAP), University of Mons-UMONS, 20 Place du Parc, B-7000 Mons, Belgium. E-mail: noemie.hergue@umons.ac.be*
[b]*Institute of Condensed Matter and Nanosciences (IMCN), Bio- and Soft Matter (BSMA), Université catholique de Louvain, Place L. Pasteur 1, B-1348 Louvain-la-Neuve, Belgium*
[c]*Laboratory for Chemistry of Novel Materials, Center of Innovation and Research in Materials and Polymers (CIRMAP), University of Mons-UMONS, 20 Place du Parc, B-7000 Mons, Belgium*
[d]*Organic Synthesis and Mass Spectrometry Laboratory, Interdisciplinary Center for Mass Spectrometry, University of Mons-UMONS, 23 Place du Parc, 7000 Mons, Belgium*

†Electronic supplementary information (ESI) available. See DOI: 10.1039/c9py00268e

mandatory to further reduce the solubility of the polymer. This can be achieved by increasing the molar mass of PTMA, as demonstrated in a recent paper.[15] To further immobilize the polymer, PTMA can be introduced in a network, cross-linked and also grafted onto or made to interact strongly with the conductive materials.[12,14,16,17] In this respect, the use of supramolecular interactions between PTMA and the conductive carbon additives allows for a high control on the polymer structure and the use of pristine conductive materials. In most of the reported studies, TEMPO units are integrated into a polymeric structure playing only the role of a matrix in order to lower the solubility or to enable interactions with the conductive carbon materials. Few examples deal with the combination between TEMPO groups and a conductive polymer backbone structure such as polypyrrole[10,18] and polythiophene[19,20] able to improve the overall charge transport.

Herein, we report on the synthesis and the electrochemical properties of diblock copolymers associating a conjugated polymer (poly(3-hexylthiophene), P3HT) and a stable radical polymer (PTMA). Using a conjugated polymer block, we are aiming: (i) to improve the overall electrode performances by increasing the charge transport properties and (ii) to take advantage of the supramolecular interactions between P3HT and CNTs[21] to immobilize PTMA and minimize capacity losses during cycling. In the previous literature, the compounds associating TEMPO and P3HT are either made by electrodeposition or chemical polymerization of a thiophene ring bearing a TEMPO unit on the 3 position,[20,22,23] or *via* the synthesis of copolymer architectures in which TEMPO units are connected through the 3 position *via* various linkers.[19] Here, we design an architecture where the two blocks (P3HT and PTMA) are linked together as a diblock structure in order to preserve the individual properties of each constituent block.

Results and discussion

Synthesis of the diblock copolymers

The first synthetic pathway considered in our study consisted in growing the polymer precursor of the PTMA block, *i.e.* a poly(2,2,6,6-tetramethyl-4-piperidyl methacrylate) (PTMPM) from a P3HT chain by atom transfer radical polymerization (ATRP) of the 2,2,6,6-tetramethyl-4-piperidyl methacrylate (TMPM) monomer (Fig. S1†).[24] In this approach, P3HT was thought to be synthesized by Grignard metathesis, a method known to prepare polymers characterized by a good control over the molar mass, the end groups and leading to narrow dispersities.[25] Ideally, the ω-chain end of the conjugated polymer should be then modified in three steps to obtain an ATRP macroinitiator able to initiate the ATRP polymerization of TMPM giving access to the targeted P3HT-*b*-PTMPM diblock copolymer. Unfortunately, P3HT is not stable during the step of oxidation required to transform the PTMPM block into PTMA (Fig. S1†). This was demonstrated by the disappearance of the single aromatic peak of thiophene at 6.98 ppm in ^{1}H NMR, by an enlargement of the SEC trace of the diblock copolymer and by a widening of its absorption peak in UV-Vis spectroscopy in agreement with an oxidation of P3HT in S-oxide as reported by Barbarella *et al.*[26,27]

To avoid such a degradation, it was needed to consider a second synthetic pathway consisting in a direct coupling reaction between two pre-synthesized and end-functionalized P3HT and PTMA blocks. This strategy relies on a copper azide–alkyne coupling cycloaddition (CuAAC) of an azide end-functionalized PTMA (N_3-PTMA) and an alkyne end-functionalized P3HT (P3HT-Alk) homopolymers.

Synthesis of the N_3-PTMA block

The synthesis of the N_3-PTMA block, depicted on Fig. 1, follows a two-step process involving the homopolymerization

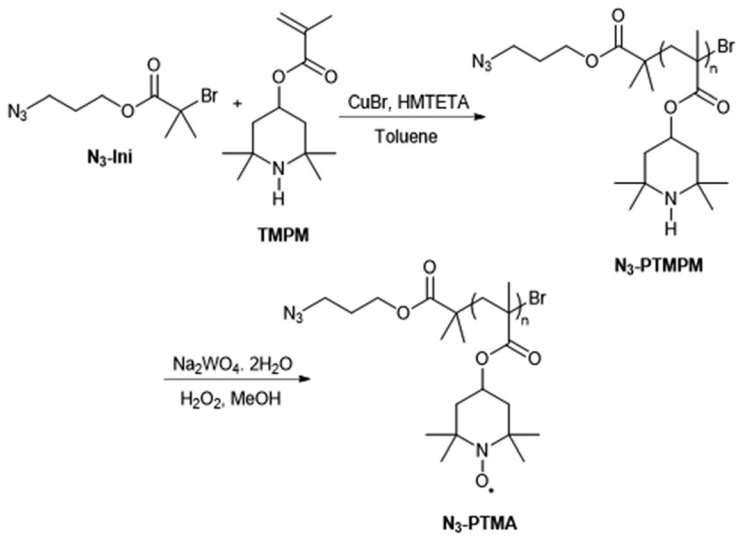

Fig. 1 Synthetic pathway to N_3-PTMAs.

of TMPM from an azide-based initiator, followed by an oxidative treatment of the secondary amine functions into nitroxide groups. Prior to the polymerization, the azide-based initiator (N_3-Ini) was prepared in a two-step process from the commercially available 3-bromo-1-propanol (Fig. S2†). The use of N_3-Ini also allows for an easy determination of the degree of polymerization (DP) by ^{1}H NMR. The homopolymerization of TMPM ($[TMPM]_0$ = 2.8 mol L^{-1}) was then performed in toluene at 50 °C using a CuBr/HMTETA catalytic complex and the N_3-based initiator ($[N_3\text{-Ini}]_0/[CuBr]_0/[HMTETA]_0$ = 1/1/2).[28] The reaction times were adjusted depending on the targeted DP. Two different N_3-PTMPM polymers were synthesized and characterized by both ^{1}H NMR and SEC analysis. Experimental DPs were of 48 and 87 while the dispersity values equaled 1.21 and 1.18, respectively. These two compounds, abbreviated as N_3-$PTMPM_{48}$ and N_3-$PTMPM_{87}$, were then oxidized with an excess of H_2O_2 in the presence of $Na_2WO_4{\cdot}2H_2O$/EDTA in methanol at 60 °C for 24 hours ($[N_3\text{-PTMPM}]_0$ = 20 g L^{-1}). The oxidation degrees of both N_3-$PTMA_{48}$ and N_3-$PTMA_{87}$ were determined by UV-visible absorption spectroscopy to be above 98% each.

Synthesis of the alkyne-P3HT block

The second block is prepared *via* a Kumada catalyst-transfer polycondensation (KCTP) on a 3-hexylthiophene-based monomer.[29] This well-known KCTP procedure allows for a controlled polymerization in terms of molar mass and dispersity.[30]

The first polymerizations were carried out onto 2-bromo-3-hexylthiophene using the 2,2,6,6-tetramethylpiperidinyl–magnesium chloride lithium chloride complex solution (TMPMgCl·LiCl) in THF (see Experimental part in ESI,† for details).[31]

The polymerizations were then quenched with an excess of ((trimethylsilyl)ethynyl)magnesium chloride to introduce a protected alkyne function as P3HT end-group. Note here that the protected alkyne quencher was used to get rid of possible alkyne–alkyne homocoupling reactions as reported by Li *et al.*[32] Under those conditions, the trimethylsilyl-protected ethynyl-terminated P3HTs are found to be stable at ambient conditions for very long periods of time, allowing the purification of the polymers by Soxhlet extractions without degradation. Intriguingly, MALDI-ToF analyses revealed that monofunctionalized P3HTs were contaminated by di-functionalized P3HTs (30%, as determined by ^{1}H NMR). The presence of di-alkyne P3HT represents a serious issue for the formation of the expected diblock copolymers and is likely to lead to a mixture of di- and undesired tri-block structures. To our own opinion, such a contamination could originate from the KCTP process possibly involving a "ring walk" of the catalyst from one end of the growing polymer chain to the other.[33]

To avoid the formation of such a mixture, a new synthetic pathway was followed and the use of a modified catalyst that does not present any "ring-walking effect" along the polymer chain was selected.[34] The preparation of pure mono-functionalized P3HTs was then achieved in THF starting from a tolyl-modified catalyst freshly prepared using TMPMgCl·LiCl (Fig. S4†). Homopolymerization of 2-bromo-3-hexylthiophene ($[3HT]_0$ = 0.1 mol L^{-1}) was achieved in THF at −4 °C using a (*o*-tolyl)Ni(dppp)Br prepared *in situ* by ligand exchange of (*o*-tolyl)Ni(PPh_3)$_2$Br by dppp (ratio 1 to 2) and 1 equivalent of TMPMgCl·LiCl. Two homopolymers were prepared targeting DPs of 30 and 36, respectively. As determined by ^{1}H NMR, experimental DPs, calculated from the intensities of the methyl peak of the tolyl group at δ 2.5 ppm and the one of the first CH_2 of the hexyl side chain at δ 2.81 ppm, were determined to be 31 and 35, respectively, in very good agreement with the targeted values. Reactions were then quenched by addition of an excess of ((trimethylsilyl)ethynyl)magnesium chloride. In order to confirm the efficiency of the end-group functionalization, MALDI mass spectrum was recorded. The spectrum presents one main distribution corresponding to 3-hexylthiophene polymer with the expected end-groups (Fig. 2, S6 and S7†). Beside the targeted P3HT end-functionalized with an *o*-tolyl on one side and a protected alkyne on the other side (red dots), deprotected polymer (blue dots) is also formed. The presence of the characteristic signals in ^{1}H NMR (Fig. S8†) also confirms that our strategy allows alkyne monofunctionalized P3HTs (named $P3HT_{31}$-PrAlk and $P3HT_{35}$-PrAlk) to be prepared.

Coupling process

Both P3HT-PrAlk were deprotected at room temperature just before the coupling reaction using 2 equivalents of tetra-*n*-butylammonium fluoride in THF for 2 hours ($[P3HT\text{-}PrAlk]_0$ = 0.47 mmol L^{-1}). The as-obtained deprotected P3HTs-Alk were then coupled with the N_3-PTMAs by CuAAC in THF (0.94 mmol L^{-1}) using copper bromide and *N*,*N*′,*N*″,*N*″-pentamethyldiethylenetriamine (PMDETA) as catalytic complex ($[CuBr]_0/[PMTETA]_0$ = 0.86) in the presence of sodium ascorbate ($[C_6H_7NaO_6]_0$ = 1.9 mmol L^{-1}) at room temperature for 1.5 hours (Fig. 3). Table 1 summarizes the experimental parameters of the P3HTs and the PTMAs involved in the coupling processes as well as the experimental parameters of the two obtained P3HT-*b*-PTMA diblock copolymers. As represented for the $P3HT_{35}$-*b*-$PTMA_{48}$ sample, SEC analysis confirms the efficiency of the coupling process by a clear shift of the elution

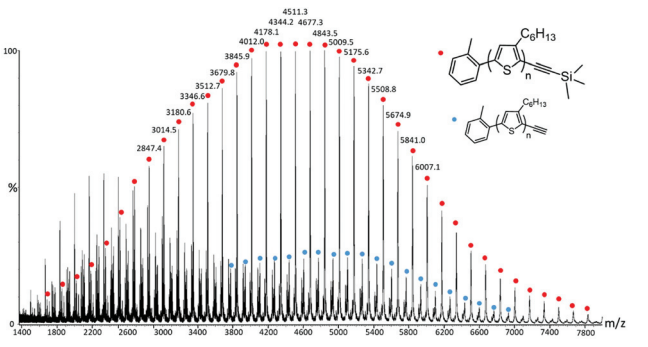

Fig. 2 MALDI-ToF spectrum of the $P3HT_{31}$-PrAlk.

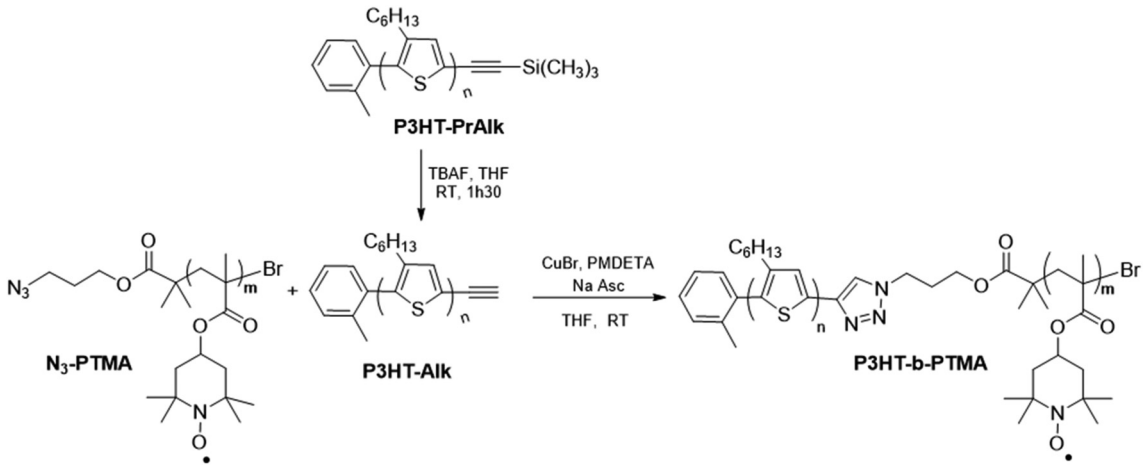

Fig. 3 Synthesis of P3HT-*b*-PTMA diblock copolymers by copper azide–alkyne coupling cycloaddition from P3HT-Alk and N_3-PTMA.

Table 1 Molecular characteristic features of the P3HT-*b*-PTMA diblock copolymers

	M_{nP3HT} [a] (g mol^{-1})	DP_{P3HT} [c]	M_{nPTMA} [b] (g mol^{-1})	DP_{PTMA} [c]	M_{ncopo} [d] (g mol^{-1})	$Đ$ [d]
$P3HT_{35}$-*b*-$PTMA_{48}$	8300	35	6900	48	17 700	1.33
$P3HT_{31}$-*b*-$PTMA_{87}$	7200	31	9900	87	11 800	1.34

[a] As determined by SEC in THF before coupling process. [b] As determined by SEC in $CHCl_3$/iPrOH/Et_3N, 94/2/4 (in volume) before coupling process. [c] Homopolymer experimental DPs determined by ^1H NMR ($CDCl_3$, 500 MHz). [d] Diblock copolymer molar mass and associated dispersity value as determined by SEC (THF).

peak as compared to the $P3HT_{35}$-PrAlk engaged for the reaction (Fig. 4 and Fig. S9†). The efficiency of both couplings was also qualitatively attested by the disappearance, after CuAAC, of the alkyne and azide groups in FTIR (Fig. S10†).

Electrochemical properties

The diblock copolymers have been blended with multi-walled carbon nanotubes (MWCNTs) to prepare electrodes for electrochemical measurements. A slurry made of a diblock copolymer/CNTs/binder mixture with a 30/60/10 wt% composition was prepared following a previously reported procedure[28] to favor interactions between the diblock copolymer and the CNTs and thus enhance the stability of the composite. CNTs were first dispersed in NMP using short pulses of ultrasonication, then a solution of the block copolymer was incorporated under sonication and the binder was added to this mixture directly before further stirring using a ball mill at 400 rpm. 400 nm-thick films were obtained by deposition with a Doctor Blade and disks were cut to be used as the cathode in a half cell, prepared in the glove box under argon atmosphere. A lithium foil has been used as anode and reference electrode. All electrochemical tests have been performed using the same electrolyte, namely $LiPF_6$ at 1 M in EC/DEC (1 : 1; v : v).

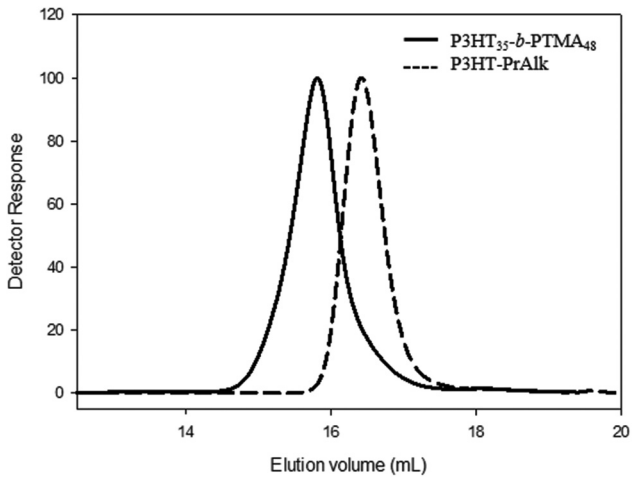

Fig. 4 SEC traces comparison between a $P3HT_{35}$-PrAlk (dash line) and its corresponding $P3HT_{35}$-*b*-$PTMA_{48}$ diblock copolymer (full line).

The electrochemical properties of the cells were first studied by cyclic voltammetry between 3.0 and 4.2 V *vs.* Li/Li^+. The P3HT-*b*-PTMA diblock copolymers exhibit the redox behavior of PTMA with a reversible oxidation peak centered at 3.6 V *vs.* Li/Li^+ (Fig. 5 and S9†). This peak is characteristic to the oxidation of the nitroxide radical ($NO^•$) into oxoammonium cation (N^+=O). This process shows a fast charge transfer characterized by a narrow peak to peak separation (40 mV) and it is fully reversible, with successive curves overlapping each other.

The retention capacity behavior of the P3HT-*b*-PTMA-based cathodes was studied over 180 cycles by galvanostatic measurements at a C-rate of C/2 (corresponding to a full charge or dis-

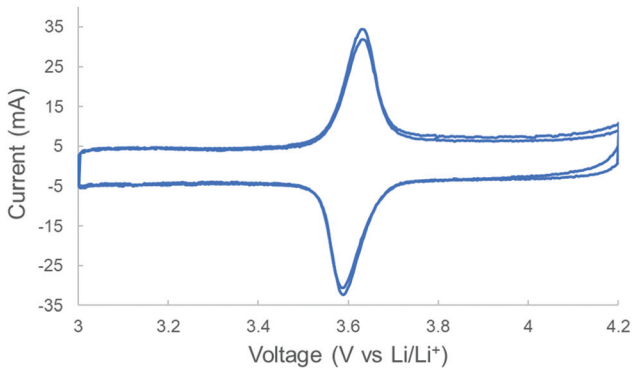

Fig. 5 Cyclic voltammogram of $P3HT_{35}$-*b*-$PTMA_{48}$ recorded at 0.1 mV s^{-1}.

charge in 2 h) between 3.0 and 4.0 V *vs.* Li/Li^+ (Fig. 6). The performances of the P3HT-*b*-PTMA diblock copolymers are compared to those of a PTMA homopolymer of a similar molar mass (DP = 84). An initial capacity drop, due to irreversible processes, is observed for the three studied polymers during the first cycles. Compared to homo-PTMA cells, which are showing a loss of 54% after 180 cycles, the P3HT-*b*-PTMA electrodes are showing more stable capacities with only 13 and 20% loss for the $P3HT_{35}$-*b*-$PTMA_{48}$ and $P3HT_{31}$-*b*-$PTMA_{87}$ diblock copolymers, respectively. After 180 cycles the capacities of the P3HT-*b*-PTMA based cells remain high. $P3HT_{31}$-*b*-$PTMA_{87}$ shows a capacity of 60 mA h g^{-1} (54% of the theoretical value) while $P3HT_{35}$-*b*-$PTMA_{48}$ demonstrates a higher capacity of 85 mA h g^{-1} (77% of the theoretical value). These results are demonstrating good performances for the block copolymers, in particular for $P3HT_{35}$-*b*-$PTMA_{48}$.

The rate performances of the block copolymer $P3HT_{35}$-*b*-$PTMA_{48}$ was investigated through charge/discharge cycles at different C rates (from C/10 to 60 C) between 3.0 and 4.2 V (Fig. 7 and 8). When increasing the current density, the capacities are decreasing. At C/10 the cathode exhibits a capacity of 116 mA h g^{-1}. This value is moderately decreased to reach a capacity of 75 mA h g^{-1} at 60 C, which is still over

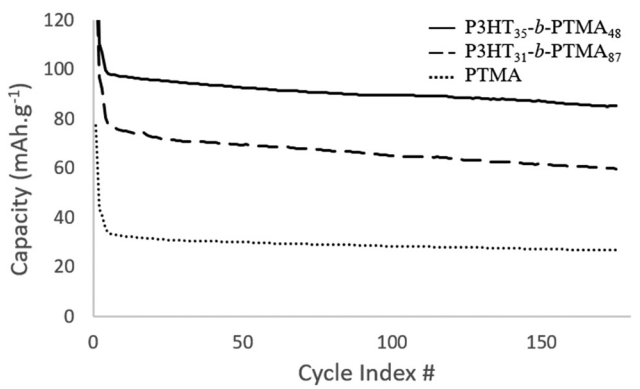

Fig. 6 Capacity retention of the P3HT-*b*-PTMA/CNTs and PTMA cathodes at C/2 rate over 180 cycles.

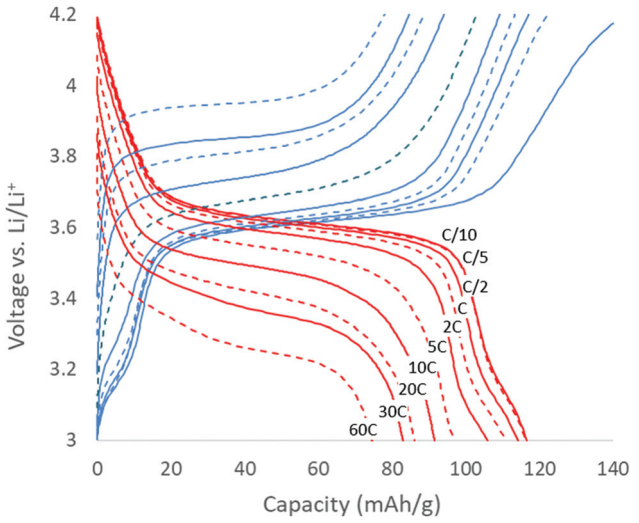

Fig. 7 Charge/discharge curves of $P3HT_{35}$-*b*-$PTMA_{48}$ from C/10 to 60 C.

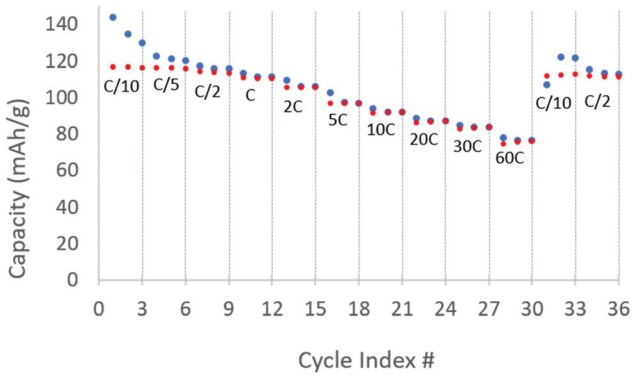

Fig. 8 Rate performances of $P3HT_{35}$-*b*-$PTMA_{48}$ from C/10 to 60 C.

67% of the nominal capacity at this high C-rate. At C/5 the curves are showing a plateau centered at 3.6 V *vs.* Li/Li^+, characteristic of PTMA. Because of the polarization, this plateau is spread when increasing the current density and keeps a symmetrical shape centered on 3.6 V *vs.* Li/Li^+. At high C-rates, the spread of the charge and discharge curves is limited, with a polarization lower than 200 mV at 60 C. This is indicating a fast charge transfer between the active species and the electrically conductive charges thanks to favorable interactions between the two components. At low C-rate, the discharge curves are showing a change of slope at around 3.2 V *vs.* Li^+/Li. In accord to our previous work,[28] such a behavior cannot be attributed to PTMA block while its origin has not been clearly identified.

At the end of the experiments, the rate was decreased, and the battery performances were recorded at C/10 and C/2; the initial performances were recovered, revealing a good stability of the cathodes.

In order to understand the effect of the conjugated polymer on the electrochemical behavior, control experiments were

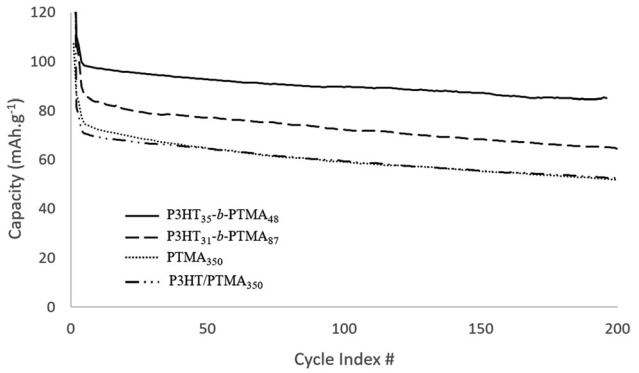

Fig. 9 Capacity retention of the block copolymer half-cells compared to PTMA and P3HT/PTMA physical blend in half-cells at C/2 rate over 200 cycles.

carried out with cathodes made from physical blends of P3HT and PTMA homopolymers, with the same P3HT/PTMA/CNTs/binder wt% ratio than previously used (10/20/60/10). The capacity retention of the resulting cells was measured using the same conditions (Fig. 9). The cathode prepared from the homo-P3HT/homo-PTMA physical blend is displaying lower performances, similar to those of homo-PTMA-based cathodes, demonstrating the interest of the block copolymer design.

Modeling of P3HT-*b*-PTMA/CNT interfaces

In order to get insight on the interactions between P3HT-*b*-PTMA and CNT, molecular modeling simulations on the polymer/CNT interface were performed. In particular, we investigated whether the two blocks can mix at the interface or whether there is selective physisorption on the nanotube wall. Molecular dynamics (MD) simulations were performed with the Biovia Materials Studio 2018 modeling package using a modified version of the Dreiding force field[35] designed to improve the description of the torsions along the P3HT backbone. This force field has been further optimized to properly describe the flexibility of the PTMA chains. In order to reduce the computational cost of the simulations, a block copolymer composition intermediate between those of the polymers reported in Table 1 was chosen. The model block copolymer consists of a P3HT block of 32 monomer units (M_n = 5300 g mol^{-1}) combined with a PTMA block of 60 monomer units (M_n = 14 600 g mol^{-1}) having a total molar mass M_n = 19 900 g mol^{-1}. As model for the CNTs, we used a rigid, periodic single wall nanotube having a diameter of 5.4 nm, representing the outer wall of a multi-wall CNT.

At first, the adsorption energy and morphology on the CNT surface of the two blocks, considered as separate polymers were investigated. A standard procedure is used for all the simulations: first the structure of the chain is relaxed in vacuum. Next, we perform a MD simulation to allow the chain to change its conformation and possibly coil. Finally, we place the chain close to the nanotube and we perform a 5 ns long MD simulation at 300 K to allow it to adsorb and diffuse on the nanotube surface.

The adsorption energy, *i.e.*, the polymer/nanotube interaction energy, E_{ads}, is calculated with eqn (1)

$$E_{ads} = E_{sys} - (E_{poly} + E_{CNT}) \quad (1)$$

where E_{sys} is the total potential energy of the polymer/CNT interface while E_{poly} and E_{CNT} are the internal potential energies for the polymer chain and the nanotube, respectively. In our model, since the nanotube was treated as a rigid body, its internal energy is zero.

In order to understand whether one block interacts preferentially with the nanotube, we have decomposed the total adsorption energy calculated for the block copolymer chain in the energetic contributions coming from the adsorption of the P3HT and PTMA blocks. The results of this energetic analysis are reported in Table 2. For comparison, the adsorption energies on the nanotube for the two blocks considered as homopolymers have also been calculated. Finally, since the blocks have different lengths and weights, we have calculated the adsorption energy per monomer unit, E_{mon}, for an easier comparison of the affinities between the blocks and the nanotube. From the energetic analysis, the P3HT block has a much stronger affinity with the nanotube than PTMA. The adsorption energy per 3HT monomer unit is more than twice as large as that of the TMA units in the homopolymers. The difference is even larger in the block copolymer, probably because the P3HT block reorganizes more efficiently when adsorbing on the CNT surface. The strength of the interaction between P3HT and CNTs stems from both π–π stacking (favorable interactions between the heteroaromatic ring and the sp^2 carbon surface) and CH–π interactions (weak hydrogen-bond interactions between the alkyl side groups and the CNT surface).[36]

Fig. 10 shows top and front views of the interface. They illustrate the fact that the block copolymer/CNT contact takes place predominantly with the P3HT block (note the quasi absence of nitrogen and oxygen atoms at the CNT surface in the front view) and that the PTMA block lies away from the surface. Overall, these simulations thus indicate that the P3HT-*b*-PTMA block copolymer chains interact with nanotubes mainly *via* the P3HT blocks, which act as strong anchor groups to keep the PTMA blocks in contact with the nanotubes. This organization is expected to both suppress the solubilization of the PTMA chains in the electrolyte and to favor the charge transfer between the redox polymer and the nanotube *via* the conjugated system. In contrast, PTMA in a mixture with P3HT does not benefit from these two features.

Table 2 Energetic analyses of the (co)polymer/CNT interfaces

System	E_{sys} (kcal mol^{-1})	E_{poly} (kcal mol^{-1})	E_{ads} (kcal mol^{-1})	E_{mon} (kcal mol^{-1} mon^{-1})
Homo-P3HT	161.7	743.7	−582.0	−18.2
Homo-PTMA	2959.3	3399.3	−440.0	−7.3
P3HT-*b*-PTMA	3268.7	3916.0	−647.3	−7.0
P3HT block	336.2	768.0	−431.8	−13.5
PTMA block	3173.5	3395.7	−222.2	−3.7

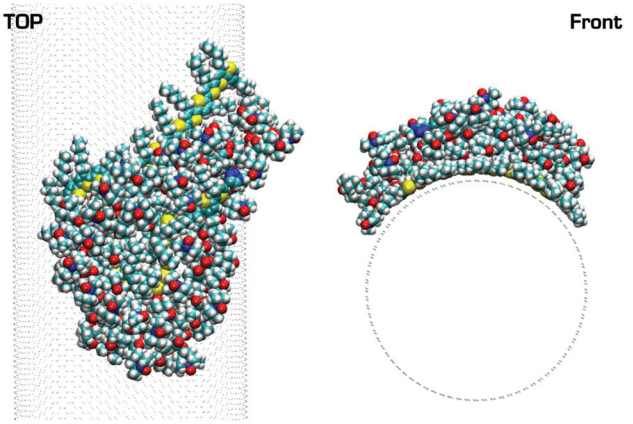

Fig. 10 Top (left) and front (right) views of the model P3HT-*b*-PTMA/CNT interface (nitrogen: blue; oxygen: red; sulfur: yellow).

Experimental section

Materials

Tetrahydrofuran (THF, VWR, 99%) was dried using an MBraun solvent purification system under N_2. 3-Bromo-1-propanol (97%, Acros), sodium azide (>99%, Merck), bromoisobutyryl bromide (98%, Aldrich), 2,2,6,6-tetramethyl-4-piperidyl methacrylate (TMPM, >98%, TCI), copper(I) bromide (CuBr, 98%, Sigma Aldrich), 1,1,4,7,10,10-hexamethyltriethylenetetramine (HMTETA, 97%, Aldrich), *N*,*N*,*N*′,*N*″,*N*″-pentamethyldiethylenetriamine (PMDETA, 99%, Aldrich), (+)-sodium L-ascorbate (Sigma), sodium tungstate dihydrate ($Na_2WO_4{\cdot}2H_2O$, ≥99%, Sigma Aldrich), hydrogen peroxide solution (50% vol, VWR), ethylenediaminetetraacetic acid disodium salt dihydrate (EDTA, ≥98%, Sigma Aldrich), tetrabutylammonium fluoride solution (1 M/THF, Acros), 1,3-bis(diphenylphosphino)-propane (dppp, 97%, Alfa Aesar), 2,5-dibromo-3-hexylthiophene (>97%, TCI), 2-bromo-3-hexylthiophene (>98%, TCI), isopropylmagnesium chloride solution (2 M/THF, Aldrich), ethynyltrimethylsilane (98%, merck), triethylamine, isopropanol and all other chemicals were used as received. Multiwall carbon nanotubes NC7000 (MWCNT) were provided by Nanocyl.

Methods

^{1}H NMR spectra were recorded at room temperature in $CDCl_3$ at a concentration of 10 mg per 0.6 mL on a Bruker AMX500 (500 MHz) equipment, with a shift reported in parts-per million downfield from tetramethylsilane used as an internal reference. Size exclusion chromatography (SEC) was performed in $CHCl_3$/iPrOH/Et_3N (for PTMA homopolymers) or in THF (for both P3HT homopolymers and corresponding block copolymers) at 30 °C using an Agilent liquid chromatograph equipped with an Agilent degasser, an isocratic HPLC pump (flow rate = 1 mL min^{-1}), an Agilent autosampler (loop volume = 100 μL, solution conc. = 1 mg mL^{-1}), an Agilent-DRI refractive index detector and three columns: a PL gel 10 μm guard column and two PL gel Mixed-D 10 μm columns (linear columns for separation of MWPS ranging from 500 to 10^7 g mol^{-1}). Poly(methyl methacrylate) standards were used for calibration for the analyses in $CHCl_3$/iPrOH/Et_3N. Polystyrene standards were used for calibration in THF. Positive-ion MALDI-Mass Spectrometry (MALDI-MS) experiments were recorded using a Waters QToF Premier mass spectrometer equipped with a Nd:YAG (third harmonic) operating at 355 nm with a maximum output of 65 μJ delivered to the sample in 2.2 ns pulses at 50 Hz repeating rate. Time-of-flight mass analyses were performed in the reflectron mode at a resolution of about 10 000. All samples were analyzed using *trans*-2-[3-(4-*tert*-butylphenyl)-2-methylprop-2-enylidene]malononitrile (DCTB) as matrix,[37] which was prepared as a 40 mg mL^{-1} solution in $CHCl_3$. This solution (1 μL) was applied to a stainless-steel target and air-dried. Polymer samples were dissolved in $CHCl_3$ to obtain 1 mg mL^{-1} solutions. Therefore, 1 μL of this solution was applied onto the target area already bearing the matrix crystals, and air-dried. For the recording of the single-stage MS spectra, the quadrupole (rf-only mode) was set to pass all the ions of the distribution, and they were transmitted into the pusher region of the time-of-flight analyzer where they were mass analyzed with 1 s integration time. Data were acquired in continuum mode until acceptable averaged data were obtained. Oxidation degree of the PTMA was determined through UV-visible titration using 4-hydroxy-2,2,6,6-tetramethylpiperidine-1-oxyl (TEMPO-OH) using the peak at 460 nm.[38]

Slurry preparation, electrode preparation, cell assembly and electrochemical measurements were achieved following the procedures described in a previous work.[28]

Synthetic procedures

Synthesis of 3-azido-1-propanol. A solution of 3-bromo-1-propanol (1.54 g, 11 mmol, 1 eq.) and NaN_3 (1.44 g, 22 mmol, 2 eq.) in 15 mL of acetonitrile is stirred under reflux for 24 h. Water is added, and sodium salts are removed. Aqueous media is extracted with ACN, then organic layer is dried over $MgSO_4$ and the solvent is removed. Residue is solubilized in Et_2O, washed twice with water. Organic layer is dried over $MgSO_4$ and solvent is removed. ^{1}H NMR ($CDCl_3$, 500 MHz): δ (ppm): 3.76 (2H, m, CH_2–OH), 3.46 (2H, t, CH_2–N_3), 1.84 (2H, m, CH_2); FT-IR (ATR, cm^{-1}): 2090 (N_3), 3349 (OH).

Synthesis of 3-azidopropyl 2-bromoisobutyrate (N_3-Ini). 3-Azido-1-propanol (750 mg, 7.4 mmol, 1 eq.) is solubilized in 20 mL of dry CH_2Cl_2. At 0 °C, Et_3N (1.25 mL, 8.9 mmol, 1.2 eq.) is added and mixture is stirred for 1 minute. Then, bromoisobutyryl bromide (1 mL, 8.1 mmol, 1.1 eq.) is added dropwise into the solution and the mixture is stirred 2 h at 0 °C, warmed up to RT and stirred 15 more hours. After filtration of the insoluble salts, the organic layer is washed 3 times with water, dried over $MgSO_4$ and the solvent is removed. Residue is solubilized in THF, Pd/C is added, and the mixture is stirred at RT for 24 hours before being filtrated onto Celite. ^{1}H NMR ($CDCl_3$, 500 MHz): δ (ppm): 4.28 (2H, CH_2–O), 3.45 (2H, CH_2–N_3), 2–1.94 (8H, m, CH_3 and CH_2); FT-IR (ATR, cm^{-1}): 2095 (N_3).

Synthesis of N_3-PTMPM. In a round-bottom flask, a solution of N_3-Ini (46 mg, 0.18 mmol, 1 eq.), TMPM (2.5 g, 11.1 mmol, 60 eq.) and HMTETA (100 μL, 0.37 mmol, 2 eq.) in 4 mL of anhydrous THF was degassed by 3 freeze–pump–thaw cyclings. In a second round-bottom flask, CuBr (26 mg, 0.18 mmol, 1 eq.) was degassed by vacuum-nitrogen cycles. After the transfer of the TMPM mixture onto CuBr, the resulting solution was degassed one more time by a freeze–pump–thaw cycle then heated at 50 °C for 2 hours. Polymerization was quenched by cooling down the reaction and exposed to the air. After filtration on basic alumina with DCM, solvent was removed. Residue was solubilized in a small amount of DCM and precipitated in cold pentane. The white solid was isolated by filtration and dried at 40 °C under vacuum (1.77 g, 69%); FT-IR (ATR, cm^{-1}): 2124 (N_3), 3390 (NH).

Synthesis of N_3-PTMA. In a two-necked round-bottom flask fitted out with a condenser, N_3-PTMPM (1 g, 4.4 mmol of NH functions, 1 eq.), $Na_2WO_4{\cdot}2H_2O$ (404 mg, 1.3 mmol, 0.28 eq.) and EDTA·2Na (260 mg, 0.7 mmol, 0.16 eq.) were solubilized in 50 mL of MeOH. The solution was stirred at 60 °C for 10 minutes before adding H_2O_2 (5 mL, 50% vol, 175 mmol, 20 eq.) dropwise over 1 h. The solution was then stirred at 60 °C for 24 h. The polymer was extracted using DCM, organic layer was washed 3 times with water, dried over $MgSO_4$ and the solvent was removed under reduced pressure. The residue was solubilized in DCM, precipitate in cold pentane, filtered and dried at 40 °C under vacuum overnight to afford an orange solid (0.87 g, 82%); FT-IR (ATR, cm^{-1}): 2099 (N_3).

Synthesis of protected alkyne-P3HT (P3HT-PrAlk). *Procedure A*: A two-necked round-bottom flask was fitted with 2-bromo-3-hexyl-5-iodothiophene (0.8 mL, 3.7 mmol) in 15 mL of dry THF. At 0 °C, iPrMgCl (1.8 mL, 3.66 mmol, 0.99 eq.) was added in one portion and solution was stirred at this temperature for 45 minutes. Then this solution was transferred onto Ni(dppp)Cl_2 (55 mg, 1×10^{-4} mol, 0.027 eq.) and polymerization was carried out for 2 hours. A freshly prepared ((trimethylsilyl) ethynyl)magnesium chloride (20 eq.) was used to quench the polymerization and the mixture was stirred for 1 hour at RT before being precipitated in MeOH. Filtration, drying under vacuum and purifications by Soxhlet extraction in MeOH and acetone. The extraction with $CHCl_3$ led to full solubilization. Solvent evaporation and reprecipitation in MeOH afford the expected polymer as a dark solid.

Procedure B: A two-necked round-bottom flask was fitted with bromo(*o*-tolyl)bis(triethylphosphine) nickel(II) (93 mg, 0.12 mmol, 1 eq.) and dppp (102 mg, 0.25 mml, 2 eq.) solubilized in 35 mL of dry THF. This solution was stirred at RT for 15 minutes. 2-Bromo-3-hexylthiophene (0.74 mL, 3.7 mmol, 30 eq.) and TMPMgCl. LiCl (3.7 mL, 3.7 mmol, 30 eq.) are added to the previous mixture and the solution is stirred at RT for 40 minutes. A freshly prepared quencher is added (2 mL, 8 eq.) and mixture is allowed to stir one hour. Precipitation in MeOH, filtration and purification by Soxhlet extraction using MeOH and acetone followed by solubilization in $CHCl_3$ and reprecipitation in MeOH afford the expected polymer as a dark solid (339 mg). FT-IR (ATR, cm^{-1}): 2136 (C≡C).

Deprotection of trimethylsilylethynyl-P3HT (P3HT-Alk). In a round-bottom flask trimethylsilylethynyl-P3HT (236 mg, M_n = 5000 g mol^{-1}, 4.72×10^{-5} mol, 1 eq.) is solubilized in 100 mL of dry THF. TBAF (95μL, 9.4×10^{-5} mol, 2 eq.) is added and resulting mixture is stirred at room temperature for 2 hours. Part of the THF is removed under reduced pressure, then 50 mL of water are added, and the mixture is extracted with 50 mL of $CHCl_3$. The as-obtained organic layer is washed 3 times with water (30 mL), dried over $MgSO_4$ and solvent is removed under reduced pressure, affording ethynyl-P3HT as a dark solid, used directly in the next step.

Typical procedure for the synthesis of P3HT-*b*-PTMA. A solution of ethynyl-P3HT (4.72×10^{-5} mol, 1 eq.), N_3-PTMA (557 mg, 4.72×10^{-5} mol, 1 eq.), sodium ascorbate (16 mg, 8×10^{-5} mol, 1.7 eq.) and PMDETA (16 μL, 7.5×10^{-5} mol, 1.6 eq.) solubilized in 50 mL of anhydrous THF was degassed by 3 freeze–pump–thaw cyclings. In a second round-bottom flask, CuBr (10 mg, 6.6×10^{-5} mol, 1.4 eq.) was degassed by vacuum-nitrogen cycles. After the transfer of the solution onto CuBr, the resulting solution was degassed one more time by a freeze–pump–thaw cycle and stirred at RT for 36 hours. Part of the THF is removed under reduced pressure, mixture is precipitated into MeOH, filtered to afford a dark solid dried at 40 °C under vacuum overnight (690 mg, 87%).

Conclusion

In this work we designed and synthesized a block copolymer associating poly(3-hexylthiophene) and poly(2,2,6,6-tetramethylpiperidinyloxy-4-yl methacrylate) (P3HT-*b*-PTMA) as active cathode material for batteries. While PTMA segments were prepared by ATRP, P3HT blocks were generated by KCTP. Both types of blocks were characterized by defined molar masses, narrow dispersities and controlled end-groups. Very efficiently, P3HT-*b*-PTMA diblock copolymers were obtained by a copper azide–alkyne coupling cycloaddition of these two end-functionalized blocks. Films of P3HT-*b*-PTMA/CNTs/binder (30/60/10 in weight) were used as cathodes and their performances in half-cells were studied. As compared to homopolymers or physical mixtures of both P3HT and PTMA, the diblock topology allows a real improvement of the capacity cells to be obtained. The electrochemical properties of the half-cells are improved by 25% for $P3HT_{31}$-*b*-$PTMA_{87}$ with a capacity of 60 mA h g^{-1} after 180 cycles (54% of theoretical capacity) and by 60% for $P3HT_{35}$-*b*-$PTMA_{48}$ (85 mA h g^{-1} after 180 cycles, 77% of theoretical capacity). The rate performances recorded between C/10 and 60 C show a decrease in capacity from 116 to 75 mA h g^{-1} (67% of the nominal capacity). The initial properties were recovered while using the initial rate at the end of the experiment, confirming the stability of the P3HT-*b*-PTMA electrodes. Molecular modeling simulations were used to investigate the block copolymer/CNT interface. Those calculations show a stronger interaction of CNTs with P3HT than with PTMA. As a consequence, the block copolymer behaves in such a way that the PTMA block is maintained

close to the CNTs *via* P3HT anchoring, which also favors electron transfer between the CNT and the redox units of PTMA *via* the conjugated block.

Conflicts of interest

There are no conflicts to declare.

Acknowledgements

The authors are grateful to the HYB2HYB and BATWAL projects from the DGO6 of the Service Public de Wallonie. Computational resources have been provided by the Consortium des Equipements de Calcul Intensif (CECI), funded by the Fonds de la Recherche Scientifique (F.R.S.-FNRS) under Grant No. 2.5020.11. O. C is FRS-FNRS Research Associate. The UMons MS laboratory acknowledges the F.R.S.-FNRS for the acquisition of the Waters QToF Premier mass spectrometer and for continuing support.

Notes and references

1 Y. Liang, Z. Tao and J. Chen, *Adv. Energy Mater.*, 2012, **2**, 742–769.
2 W. Huang, in *Polymer science: research advances, practical applications and educational aspects*, Formatex Research Center, 2016, pp. 566–578.
3 Y. Tang, Y. Zhang, W. Li, B. Ma and X. Chen, *Chem. Soc. Rev.*, 2015, **44**, 5926–5940.
4 A. S. Arico, P. Bruce, B. Scrosati, J.-M. Tarascon and W. van Schalkwijk, *Nat. Mater.*, 2005, **4**, 366–377.
5 T. Janoschka, M. D. Hager and U. S. Schubert, *Adv. Mater.*, 2012, **24**, 6397–6409.
6 T. Jähnert, B. Häupler, T. Janoschka, M. D. Hager and U. S. Schubert, *Macromol. Chem. Phys.*, 2013, **214**, 2616–2623.
7 T. Jähnert, B. Häupler, T. Janoschka, M. D. Hager and U. S. Schubert, *Macromol. Rapid Commun.*, 2014, **35**, 882–887.
8 K.-A. Hansen and J. P. Blinco, *Polym. Chem.*, 2018, **9**, 1479–1516.
9 H. Nishide, S. Iwasa, Y.-J. Pu, T. Suga, K. Nakahara and M. Satoh, *Electrochim. Acta*, 2004, **50**, 827–831.
10 L. Xu, F. Yang, C. Su, L. Ji and C. Zhang, *Electrochim. Acta*, 2014, **130**, 148–155.
11 C.-H. Lin, J.-T. Lee, D.-R. Yang, H.-W. Chen and S.-T. Wu, *RSC Adv.*, 2015, **5**, 33044–33048.
12 B. Ernould, O. Bertrand, A. Minoia, R. Lazzaroni, A. Vlad and J.-F. Gohy, *RSC Adv.*, 2017, **7**, 17301–17310.
13 W. Guo, Y.-X. Yin, S. Xin, Y.-G. Guo and L.-J. Wan, *Energy Environ. Sci.*, 2012, **5**, 5221–5225.
14 K. Zhang, Y. Hu, L. Wang, M. J. Monteiro and Z. Jia, *ACS Appl. Mater. Interfaces*, 2017, **9**, 34900–34908.
15 K. Zhang, Y. Hu, L. Wang, J. Fan, M. J. Monteiro and Z. Jia, *Polym. Chem.*, 2017, **8**, 1815–1823.
16 B. Ernould, M. Devos, J.-P. Bourgeois, J. Rolland, A. Vlad and J.-F. Gohy, *J. Mater. Chem. A*, 2015, **3**, 8832–8839.
17 Y. Li, Z. Jian, M. Lang, C. Zhang and X. Huang, *ACS Appl. Mater. Interfaces*, 2016, **8**, 17352–17359.
18 L. Xu, P. Guo, H. He, N. Zhou, J. Ma, G. Wang, C. Zhang and C. Su, *Ionics*, 2017, **23**, 1375–1382.
19 C.-H. Lin, C.-M. Chau and J.-T. Lee, *Polym. Chem.*, 2012, **3**, 1467–1474.
20 F. Li, D. N. Gore, S. Wang and J. L. Lutkenhaus, *Angew. Chem., Int. Ed.*, 2017, **56**, 9856–9859.
21 F. Boon, S. Desbief, L. Cutaia, O. Douhéret, A. Minoia, B. Ruelle, S. Clément, O. Coulembier, J. Cornil, P. Dubois and R. Lazzaroni, *Macromol. Rapid Commun.*, 2010, **31**, 1427–1434.
22 M. Aydin and B. Esat, *J. Solid State Electrochem.*, 2015, **19**, 2275–2281.
23 M. Aydın, B. Esat, Ç. Kılıç, M. E. Köse, A. Ata and F. Yılmaz, *Eur. Polym. J.*, 2011, **47**, 2283–2294.
24 M. C. Stefan, M. P. Bhatt, P. Sista and H. D. Magurudeniya, *Polym. Chem.*, 2012, **3**, 1693–1701.
25 R. H. Lohwasser and M. Thelakkat, *Macromolecules*, 2011, **44**, 3388–3397.
26 G. Barbarella, L. Favaretto, M. Zambianchi, O. Pudova, C. Arbizzani, A. Bongini and M. Mastragostino, *Adv. Mater.*, 1998, **10**, 551–554.
27 G. Barbarella, O. Pudova, C. Arbizzani, M. Mastragostino and A. Bongini, *J. Org. Chem.*, 1998, **63**, 1742–1745.
28 N. Hergué, B. Ernould, A. Minoia, R. Lazzaroni, J.-F. Gohy, P. Dubois and O. Coulembier, *Batteries Supercaps*, 2018, **1**, 102–109.
29 A. Kiriy, V. Senkovskyy and M. Sommer, *Macromol. Rapid Commun.*, 2011, **32**, 1503–1517.
30 R. S. Loewe, S. M. Khersonsky and R. D. McCullough, *Adv. Mater.*, 1999, **11**, 250–253.
31 S. Tanaka, S. Tamba, D. Tanaka, A. Sugie and A. Mori, *J. Am. Chem. Soc.*, 2011, **133**, 16734–16737.
32 Z. Li, R. J. Ono, Z.-Q. Wu and C. W. Bielawski, *Chem. Commun.*, 2011, **47**, 197–199.
33 R. Tkachov, V. Senkovskyy, H. Komber, J.-U. Sommer and A. Kiriy, *J. Am. Chem. Soc.*, 2010, **132**, 7803–7810.
34 H. A. Bronstein and C. K. Luscombe, *J. Am. Chem. Soc.*, 2009, **131**, 12894–12895.
35 Y. Olivier, D. Niedzialek, V. Lemaur, W. Pisula, K. Müllen, U. Koldemir, J. R. Reynolds, R. Lazzaroni, J. Cornil and D. Beljonne, *Adv. Mater.*, 2014, **26**, 2119–2136.
36 A. Beigbeder, M. Linares, M. Devalckenaere, P. Degée, M. Claes, D. Beljonne, R. Lazzaroni and P. Dubois, *Adv. Mater.*, 2008, **20**, 1003–1007.
37 J. De Winter, G. Deshayes, F. Boon, O. Coulembier, P. Dubois and P. Gerbaux, *J. Mass Spectrom.*, 2011, **46**, 237–246.
38 O. Bertrand, B. Ernould, F. Boujioui, A. Vlad and J.-F. Gohy, *Polym. Chem.*, 2015, **6**, 6067–6072.

